

Growth of Strontium-doped Lanthanum Chromium Manganite/Gadolinium-doped Ceria (LSCM/GDC) Nanocomposite Particles as Ni-free Solid Oxide Fuel Cell Anode Material

Yoshiki Inaba ^{*1}, Kazuyoshi Sato ^{*1}, Naokatsu Kannari ^{*1}, Hiroya Abe ^{*2}
Anna Sciazko ^{*3}, Naoki Shikazono ^{*3}

^{*1}Division of Environmental Engineering Science, Graduate School of Science and Technology, Gunma University

^{*2}Joining and Welding Research Institute, Osaka University

^{*3}Institute of Industrial Science, The University of Tokyo

Abstract : Strontium-doped lanthanum chromium manganite /gadolinium-doped ceria (LSCM/GDC) nanocomposite particles were grown by means of a colloidal processing based bottom-up approach as Ni-free anode material of solid oxide fuel cells. X-ray diffraction analysis indicates that GDC nanocrystals dispersed in the aqueous medium plays as nucleation site of non-crystalline LSCM precursor, then the precursor transformed into crystalline perovskite phase at 1000 °C. Scanning transmission electron microscopy with energy dispersed X-ray spectroscopy reveals that the composite particles are composed of uniformly dispersing nano-sized LSCM and GDC particles with narrow size distributions. The nanostructured porous anode with the grains of <100 nm diameter was successfully fabricated using the nanocomposite particles after sintering at 1100 °C. The nanocomposite anode showed good hydrogen oxidation reaction performance competitive to Ni-based cermet.

Key Words : Strontium-doped Lanthanum Chromium Manganite (LSCM), Gadolinium-doped Ceria (GDC), Colloidal processing, Nanocomposite anode, Solid oxide fuel cells (SOFCs)

1 . Introduction

Solid oxide fuel cells (SOFCs) are one of the promising future power sources because of their high energy conversion efficiency with clean exhaust.

Further improvement of energy conversion efficiency has been demanded, recently. Ideally, the efficiency is maximized when supplied fuel is utilized completely in the SOFC stack. However, the fuel utilization is restricted in most widely used Ni-based cermet anode in order to prevent oxidation of metallic Ni by H₂O evolved through hydrogen oxidation reaction (HOR) ¹⁾.

Developments of alternative anode materials have been investigated extensively in the last two decades in order to overcome the redox-stability issue. Perovskite and related oxides, including La_{1-x}Sr_xCr_{0.5}Mn_{0.5}O₃ (LSCM) ^{2)~5)}, La-doped SrTiO₃ ⁶⁾, (PrBa)_{0.95}(Fe_{0.9}Mo_{0.1})₂O_{5+δ} ⁷⁾, and Sr₂MgMoO_{6-δ} ⁸⁾ have been proposed as post Ni-based cermet anode materials. Among them LSCM is one of the

promising candidates from the viewpoints of high redox stability, good chemical and mechanical compatibility with electrolyte, good coking resistance and sulfur poisoning tolerance ²⁾. However, the HOR performance of LSCM is still far away from the Ni-based cermet due to less HOR activity at each reaction site and less electrical and oxide ion conductivity ³⁾.

The addition of mixed ionic-electronic conductor (MIEC) such as gadolinium-doped ceria (GDC) ⁵⁾ into electronic conductive LSCM, so-called LSCM/GDC composite anode seems effective way to recover less HOR activity ²⁾. However, performance gain would be limited by just adding GDC, and further microstructural refinement is needed.

Fabrication of the LSCM/GDC nanocomposite anode seems an effective approach to improve HOR performance through significant increase of reaction site density. Recently, we have been developed a colloidal processing based bottom-up approach for the synthesis of

nanocomposite particles⁹⁾. In the present study, we have attempted to grow LSCM/GDC nanocomposite particles by this approach for nano-structured LSCM/GDC composite anode with competitive HOR performance to Ni-based cermet.

2. Experimental procedure

2.1 Growth of LSCM/GDC nanocomposite particles

LSCM/GDC nanocomposite particles with the target GDC content of 50 wt% were grown in the sequence shown in Figure 1. The specific feature of this approach is induction of heterogeneous nucleation of LSCM precursor at the surface of colloidal GDC nanocrystals⁹⁾. The GDC nanocrystals (approximately 4 nm diameter) dispersed in a basic aqueous solution (pH10 with CO_3^{2-}) was used as GDC source¹⁰⁾. Aqueous nitrate solutions of La^{3+} , Sr^{2+} , Cr^{3+} , and Mn^{2+} with a stoichiometric composition were added to the GDC nanocrystals aqueous solution with vigorous stirring, and then a blue-grey precipitates were formed immediately in the mixed solution. The precipitates were separated from the solution,

and then washed with an aqueous solution to remove unwanted species, followed by freeze-drying. The dried precursor was heat-treated at 1000 °C for 6 h in a muffle furnace to convert the precursor into LSCM/GDC nanocomposite particles.

2.2 Characterization of the nanocomposite particles

Thermal decomposition behavior of the precursor was characterized by thermogravimetry coupled with differential thermal analysis (TG-DTA; TGD-9700, ULVAC). Phase evolution by heat treatment was characterized by X-ray diffraction (XRD; SmartLab, Rigaku) using $\text{Cu-K}\alpha$ radiation in the 2θ range 20–60°. The bulk composition of the composite particles was analyzed by inductively coupled plasma optical emission spectroscopy (ICP-OES, SPECTROBLUE, Hitachi High-Tec). Morphology and phase distributions of the nanocomposite particles were characterized by a scanning transmission electron microscopy (STEM; JEM-2100F, JEOL, Japan) coupled with an energy-dispersive X-ray spectroscopy (EDS; JED-2300T, JEOL, Japan).

2.3 Fabrication of the nanocomposite anode

A symmetric button cell with the electrode area of 0.28 cm^2 were employed to evaluate HOR performance of the LSCM/GDC nanocomposite anode. A dense yttria-stabilized zirconia (YSZ) pellet was used as the electrolyte. The LSCM/GDC paste was prepared from the nanocomposite particles calcined at 1000 °C followed by ball milling for 12 h, and vehicle containing a binder, dispersant, and solvent. The cathode and anode were fabricated by screen-printing LSCM/GDC paste onto both sides of the YSZ pellet, followed by sintering at 1100 °C for 2 h. As the current collection layer, Pt paste was applied onto both electrodes, followed by heat treatment at 900 °C for adhesion. Pt wire was applied onto circumference of the electrolyte pellet as reference electrode. Pt paste was applied onto reference electrode to improve the contact.

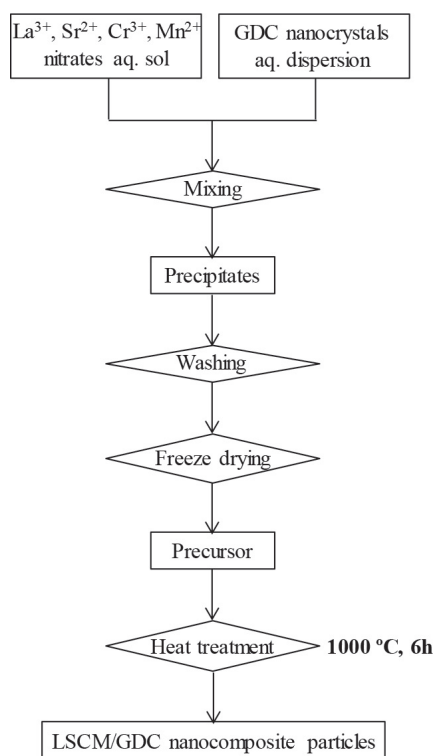


Figure 1 Growth scheme of LSCM/GDC nanocomposite particles.

2.4 HOR performance evaluation and microstructural characterization of LSCM/GDC nanocomposite anode

The HOR performance of the LSCM/GDC nanocomposite anode was examined by electrochemical impedance spectroscopy (EIS) at 800 °C. Pseudo air (21 %O₂-79 %N₂) was supplied to cathode and reference electrode, while 3%-humidified H₂ gas to anode with the flowing rate of 100 sccm. The EIS spectra were recorded between the anode and reference electrode using a frequency response analyzer with a potentiostat (Versa STAT 3, Princeton Applied Research) in the frequency range from 10⁻¹ to 10⁵ Hz under the open-circuit condition with applied amplitude of 10mV. The microstructure of the anode was observed by a scanning electron microscopy (SEM; JSM-6700F, JEOL).

3. Results and discussion

The LSCM phase of La_{0.79}Sr_{0.26}Cr_{0.48}Mn_{0.47}O_{3-d}, and GDC content of 47 wt% were estimated from the bulk composition analyzed by ICP-OES. Nearly stoichiometric composition of LSCM and small deviation of GDC content from the target evidenced successful co-precipitation of LSCM precursor with GDC nanocrystals in the present approach.

Figure 2 shows TG-DTA profiles of LSCM/GDC precursor. Some specific weight losses coupled with exothermic and endothermic events appear at several points

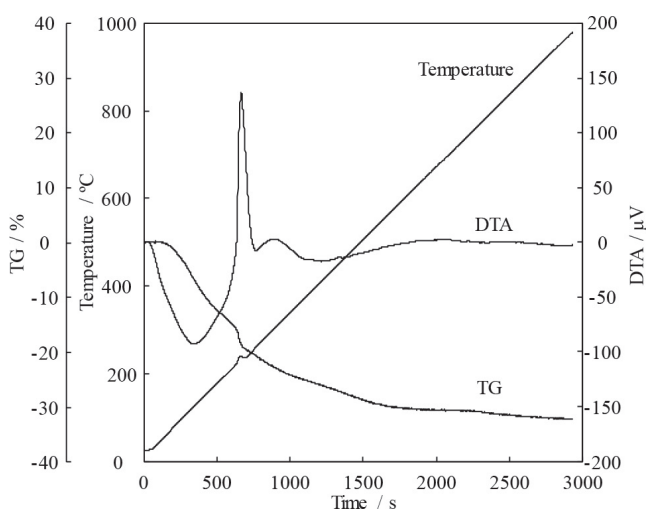


Figure 2 TG-DTA profiles of LSCM/GDC precursor.

over the temperature range. Significant weight loss with broad endothermic peak at below 200 °C is mainly attributed to removal of physisorbed water. Steep weight loss coupled with sharp exothermic peak at around 240 °C suggests the burnout of organic species adsorbed on GDC nanocrystals, which is typically observed in oxides grown by a surface-capping assisted hydrothermal method¹¹. Subsequent gradual weight loss with broad endothermic peak up to around 700 °C can be attributed to decomposition of hydroxides and carbonates. Finally, weight change almost completed at 1000 °C, and approximately 32 % of weight was lost.

Figure 3 shows XRD patterns of the sample before and after calcination. Only the broad peaks associated with GDC nanocrystals were observed in the precursor, indicating non-crystalline phase of LSCM precursor. The sample composed of LSCM and GDC phases without any other phase was obtained at 1000 °C. It is reported that heat treatment at and above 1100 °C is required to form pure LSCM phase without any impurity phases such as La₂O₃ and SrCrO₄ in the combustion synthesis^{3), 12)}. The fact suggests that the constituent elements of LSCM were uniformly distributing entire the precursor as suggested by non-crystalline structure, and those were incorporated into final product after thermal decomposition without forming intermediate phases.

Figure 4 shows STEM and corresponding elemental distribution mappings by EDS of the nanocomposite particles after heat treatment at 1000 °C. STEM image

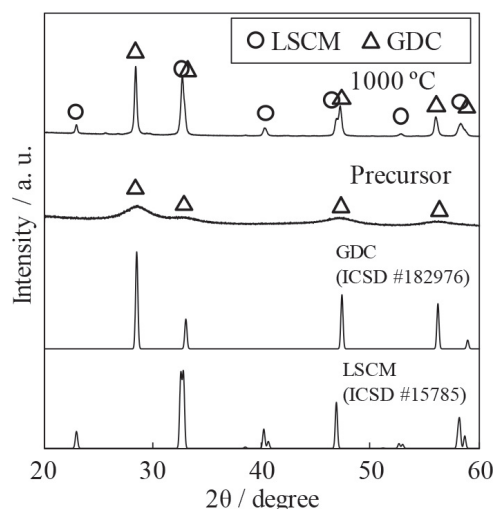


Figure 3 XRD patterns of the precursor and the LSCM/GDC nanocomposite particles after heat treatment at 1000°C.

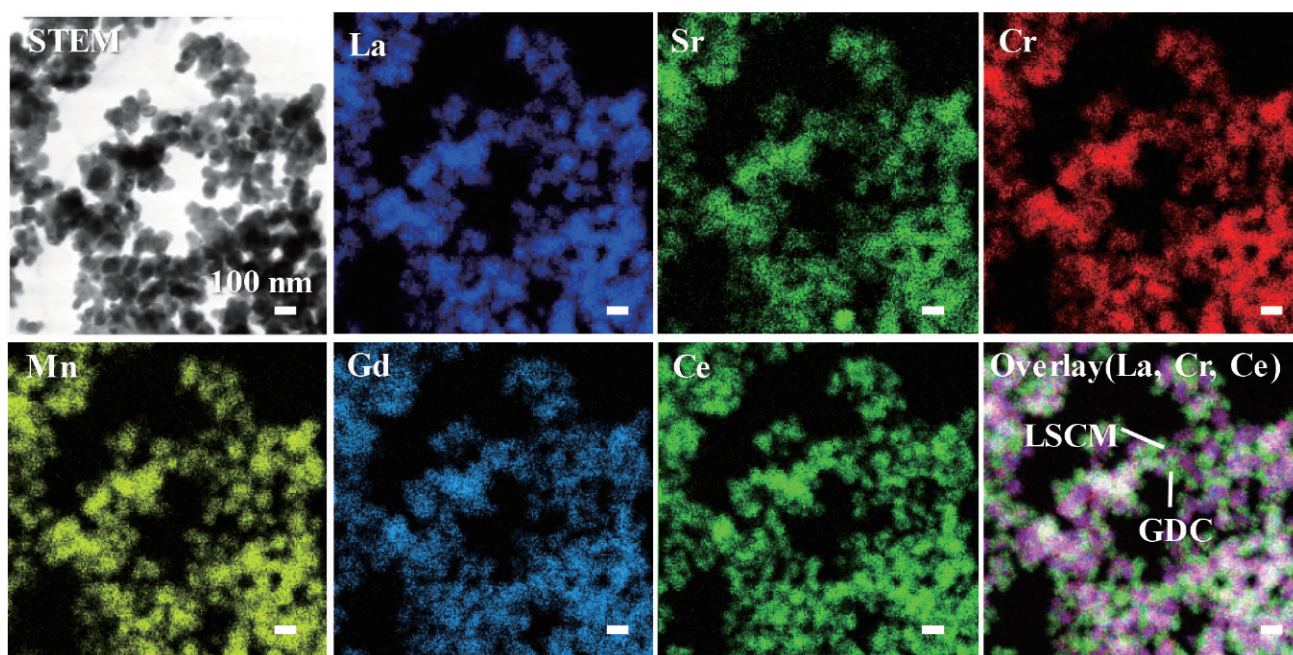


Figure 4 STEM and corresponding EDS images of LSCM/GDC nanocomposite particles after heat treatment at 1000 °C.

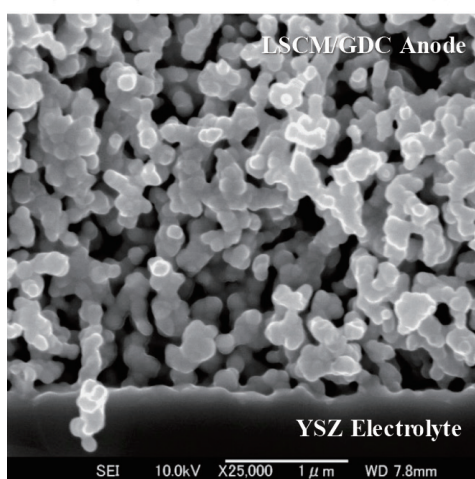


Figure 5 Cross-sectional SEM image of LSCM/GDC nanocomposite anode/YSZ electrolyte interface.

showed that the particles has the size of <100 nm diameters, and has narrow size distribution. EDS mappings indicate no significant segregation of constituent elements. Overlay image reveals that LSCM and GDC phases are uniformly distributing in the nanocomposite and are placed alternately. These results prove successful growth of LSCM/GDC nanocomposite particles according to the strategy of heterogeneous nucleation of LSCM precursors induced by GDC nanocrystals coexisting in the solution.

Figure 5 shows the cross-sectional SEM image of

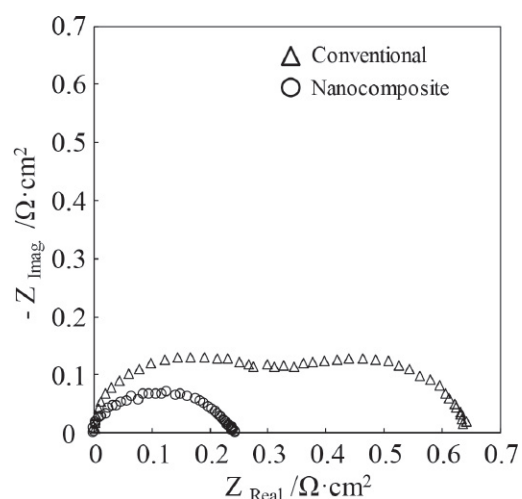


Figure 6 EIS spectra of LSCM/GDC anodes from the nanocomposite particles and mechanically mixed particles at 800 °C.

LSCM/GDC anode fabricated using the nanocomposite particles sintered at 1100 °C. The nanostructured anode with the grains of <100 nm diameter and uniform porous structure was successfully fabricated. This can be attributed to prevented grain growth and densification during sintering by uniformly distributing hetero-phases in the nanocomposite particles as shown in Fig.4.

Figure 6 shows EIS spectra of LSCM/GDC anode at 800 °C. The data of LSCM/GDC anode made from commercial powder mixture prepared through ball-milling

was also shown for comparison. Ohmic contribution was omitted in this figure for the sake of comparison of the area-specific polarization resistance (ASR) for HOR. ASR of the nanocomposite anode was $0.23 \Omega \cdot \text{cm}^2$, and was approximately 60% lower than that of conventional anode. The HOR performance of the nanocomposite anode is competitive to Ni-YSZ cermet anode of $0.36 \Omega \cdot \text{cm}^2$ ¹³⁾. The high performance of the Ni-free LSCM/GDC nanocomposite anode is attributed to the significantly higher HOR site density as evaluated elsewhere¹⁴⁾.

4. Summary

Nano-structured LSCM/GDC nanocomposite anode was successfully fabricated from the nanocomposite particles grown with the present colloidal processing based bottom-up approach. The Ni-free composite anode showed good HOR performance competitive to Ni-based cermet anode, which is attributed to the significantly higher reaction site density.

Acknowledgement

This work was supported by the JSPS KAKENHI Grant Number 18H01376 and 18K04691. This work was performed under the Cooperative Research Program of Institute for Joining and Welding Research Institute, Osaka University.

References

- 1) S. Futamura, Y. Tachikawa et al.: Alternative Ni-Impregnated Mixed Ionic-Electronic Conducting Anode for SOFC Operation at High Fuel Utilization, *J. Electrochem. Soc.*, **164**, F3055-F3063 (2017)
- 2) S. Tao, T. S. Irvine : A redox-stable efficient anode for solid-oxide fuel cells, *Nature Mater.*, **2**, 320-323 (2003)
- 3) S. Tao, T. S. Irvine : Synthesis and characterization of $(\text{La}_{0.75}\text{Sr}_{0.25})\text{Cr}_{0.5}\text{Mn}_{0.5}\text{O}_{3-\delta}$, a redox-stable, efficient perovskite anode for SOFCs, *J. Electrochem. Soc.*, **151**, A252-A259 (2004)
- 4) R. Akama, T. Okabe, et al.: Fabrication of a micropatterned composite electrode for solid oxide fuel cells via ultraviolet nanoimprint lithography, *Microelectron. Eng.*, **225**, 111277 (2020)
- 5) A. Sciazko, J. Kubota, et al.: Microstructure and Performance of Ni-free Nano $\text{La}_{0.75}\text{Sr}_{0.25}\text{Cr}_{0.5}\text{Mn}_{0.5}\text{O}_3 - \text{Gd}_{0.2}\text{Ce}_{0.8}\text{O}_x$ Composite Anode, *ECS trans.*, **103**, 2233-2243 (2021)
- 6) X.W. Zhou, N. Yan, et al.: Progress in La-doped Sr-TiO₃ (LST)-based anode materials for solid oxide fuel cells, *RSC Adv.*, **4**, 118-131 (2014)
- 7) H. Ding, Z. Tao, et al.: A High-Performing Sulfur-Tolerant and Redox-Stable Layered Perovskite Anode for Direct Hydrocarbon Solid Oxide Fuel Cells, *Sci. Rep.*, **5**, 18129 (2015)
- 8) D. Marrero-Lopez, J. Peña-Martínez, et al.: Redox behavior, chemical compatibility and electrochemical performance of $\text{Sr}_2\text{MgMoO}_{6-\delta}$ as SOFC anode, *Solid State Ion.*, **180**, 1672-1682 (2010)
- 9) K. Sato, C. Iwata, et al.: Highly accelerated oxygen reduction reaction kinetics in colloidal-processing-derived nanostructured lanthanum strontium cobalt ferrite/gadolinium-doped ceria composite cathode for intermediate-temperature solid oxide fuel cells, *J. Power Sources*, **414**, 502-508 (2019)
- 10) K. Sato, M. Arai, et al.: Surface Capping-Assisted Hydrothermal Growth of Gadolinium-Doped CeO₂ Nanocrystals Dispersible in Aqueous Solutions, *Langmuir*, **30**, 12049-12056 (2014)
- 11) K. Sato, H. Abe and S. Ohara: Selective Growth of Monoclinic and Tetragonal Zirconia Nanocrystals, *J. Am. Chem. Soc.*, **132**, 2538-2539 (2010)
- 12) I. Jung, D. Lee, et. al: LSCM-YSZ nanocomposites for a high performance SOFC anode, *Ceram. Inter.*, **39**, 9753-9758 (2013)
- 13) K. Sato, G. Okamoto, et al.: NiO/YSZ nanocomposite particles synthesized via co-precipitation method for electrochemically active Ni/YSZ anode, *J. Power Sources*, **193**, 185-188 (2009)
- 14) A. Sciazko, R. Yokoi, et al.: Evaluation of Strontium Doped Lanthanum Chromium Manganite (LSCM) and Gadolinium Doped Ceria (GDC) Anode with Different Compositions, *ECS trans.*, **91**, 1711-1720 (2019)